Programmable wave-domain computing in wireless communications

Philipp del Hougne, Marco Di Renzo, Andrea Alù, Tie Jun Cui, Yonina Eldar, Nader Engheta, Wenjun Hu, Aydogan Ozcan

Programmable wave-domain computing in wireless communications

Philipp del Hougne[1,2,*], Marco Di Renzo[3,4], Andrea Alù[5], Tie Jun Cui[6], Yonina Eldar[7], Nader Engheta[8], Wenjun Hu[9], Aydogan Ozcan[10]

[1] CNRS, IETR – Univ Rennes, France
[2] Aalto University, Finland
[3] CNRS, L2S – CentraleSupélec, France
[4] King's College London, UK
[5] CUNY, USA
[6] Southeast University, China
[7] Weizmann Institute, Israel
[8] University of Pennsylvania, USA
[9] Yale University, USA
[10] UCLA, USA
[*] philipp.del-hougne@univ-rennes.fr

Abstract

Future wireless networks must achieve large gains in data rate, energy efficiency and latency while integrating sensing and computation. Programmable wave-domain computing (pWDC), which processes signals directly through reconfigurable wave–matter interactions, offers a way to offload part of this burden from electronic processors. In this Perspective, we review historical roots and recent work on pWDC and discuss its promise and challenges. We focus on three challenges: prototype-aware runtime optimization of pWDC hardware, enriching functionalities beyond linear continuous-wave operation, and integrating pWDC into network-level resource management. Finally, we outline open questions regarding expressivity, practicality, and security that will arise in the transition of pWDC to real-life deployment in future wireless infrastructures.

1. Introduction

Current wireless communications infrastructure heavily relies on digital signal processing. Next-generation wireless systems aim for at least 10X improvements in data rate, energy efficiency, and latency, and to integrate communications with sensing. To achieve these ambitious goals, offloading specific-purpose computations to the wave domain is emerging as a technological enabler. Wave-domain computing (WDC) broadly refers to information processing that occurs at least partially based on the interactions of physical waves (for instance, microwaves, light, or sound) with systems (for instance, metamaterials or radio environments). WDC has a long tradition dating back to the dawn of computing, but the astonishing rate of improvement of general-purpose electronic processors has thus far thwarted practical needs for WDC. Instead of rivaling electronics for general-purpose computing, recent interest in WDC targets specific-purpose operations that strategically leverage the unique benefits of wave-matter interactions related to bandwidth, parallelism, and power consumption[1]. Over the last decade, these concepts have matured thanks to advances in engineered materials and wave control[2] – see Fig.1 for a timeline of selected milestones. In particular, advances in reconfigurable metamaterials[3] have established the required hardware for *programmable* WDC (pWDC). pWDC enables deterministic adjustments of the WDC functionality during runtime. Now, given the pressing needs of next-generation wireless systems, we see a strong opportunity for pWDC to transition to real-world applications in wireless communications.

In this Perspective, we begin by introducing the fundamental concepts of pWDC and providing a historical overview of various disjoint origins of WDC in diverse research communities. With a focus on pWDC in wireless systems, we explain physics-consistent system modeling and contemporary efforts to maximize wave-domain flexibility. Then, we provide an in-depth examination of three key challenges that need to be solved to enable the transition of pWDC into real-life deployments in wireless systems.

First, what are the most promising paradigms for optimizing the configuration of programmable wave-domain infrastructure for a desired functionality in situ? This question spans from overcoming issues with model-reality mismatch all the way to possible embodiments of decentralized self-configuration for pWDC hardware.

Second, how far beyond linear operations on time-harmonic signals can we go? While WDC does not aim at general-purpose computing, features like non-linearity and memory may be very valuable assets. Their implementations are open challenges, and existing ideas imply important trade-offs between increased pWDC expressivity and metrics like speed and energy consumption.

Third, beyond the traditional scopes of wave-matter control and signal processing, what runtime control plane is needed to orchestrate pWDC-empowered wireless networks? For instance, what could a dedicated operating system look like?

We close with a brief discussion of additional open questions in the realms of expressivity, practicality, and security that will arise in the transition of pWDC from academic research to real-life deployment.

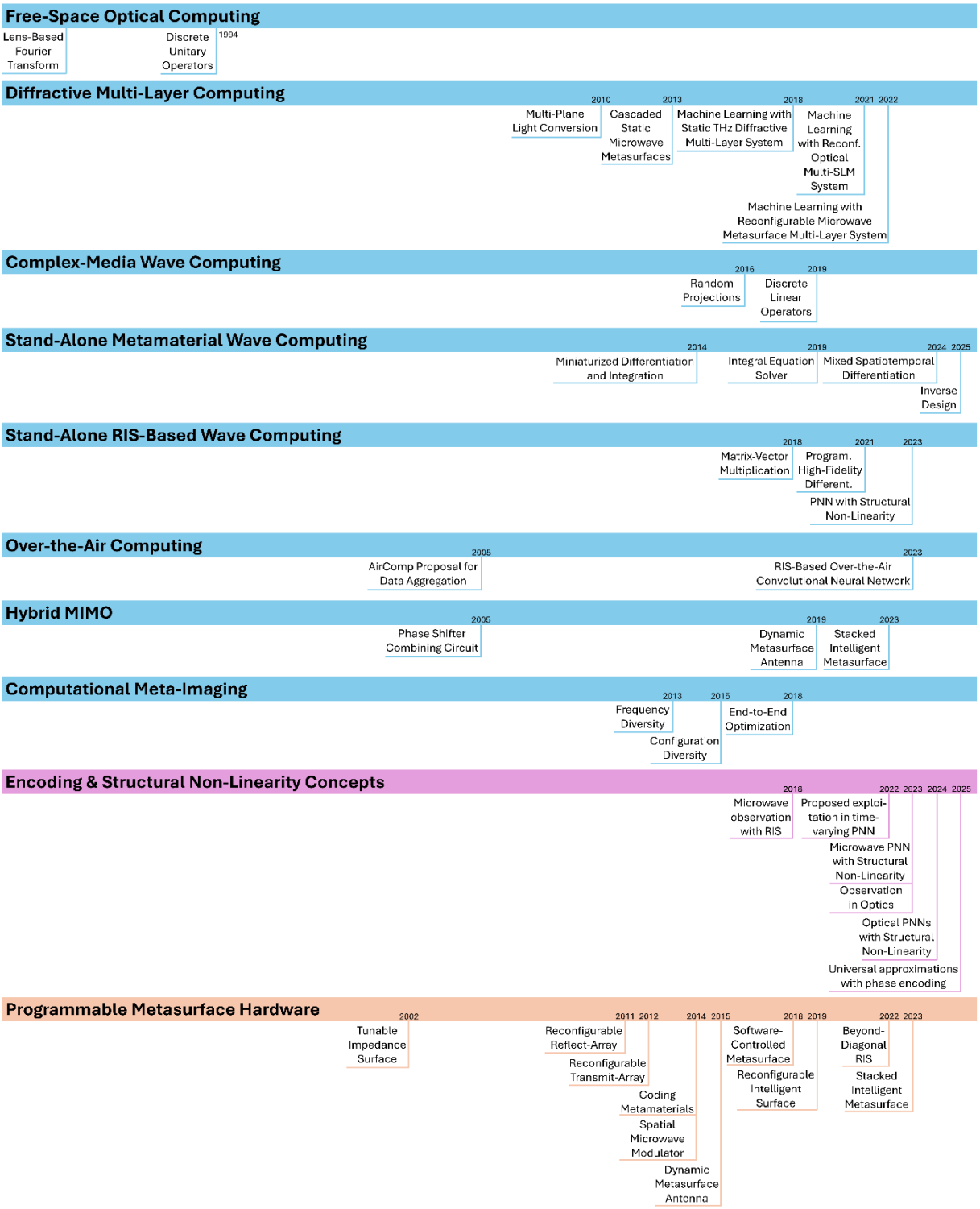

Figure 1: Timeline of selected milestones in WDC. *Corresponding references by row: free-space optical computing[4]; diffractive multi-layer computing[5–10]; complex-media wave computing[11,12]; stand-alone metamaterial wave computing[13–16]; stand-alone RIS-based wave computing[17–19]; over-the-air computing[20,21]; hybrid MIMO[22–24]; computational meta-imaging[25–27]; encoding and structural non-linearity concepts[17,28,19,29–33] (see Sec. 3); programmable metasurface hardware[34–36,3,37,26,38–41].*

2. Principles and historical origins of pWDC

WDC relies on the fact that a system's transfer function – the mapping from the impinging wavefront to the scattered wavefront – can be viewed as realizing a mathematical operation on the impinging wavefront. A basic example thereof is a lens, which is a linear optical component that implements a Fourier transform (in the appropriate Fourier plane). More elaborate examples of WDC in free-space optics have been explored for many decades, including convolution[42], wavelet transforms[43], and discrete unitary operators[4]. Advances in metamaterial engineering have enabled the miniaturization, customization, and reconfigurability of WDC. For example, a stacked metamaterial[13] or an ultrathin metasurface[44] can be designed to perform spatial differentiation, integration or convolution. Moreover, desired linear optical operations can be implemented in a static or programmable manner based on cascaded diffractive layers[5–10,45] or integrated photonic systems[46–48]. Furthermore, random scattering media can implement large-scale random projections[11] or, combined with spatial light modulators, desired linear transformations[12].

Analogous concepts also exist for wireless systems operating in the radiofrequency (RF) regime. Related to random projections through optical scattering media[11] are over-the-air computations in wireless sensor networks[20,49–51]. In this context, the uncontrolled radio environment that connects the sensor nodes to the sink node can be viewed as an over-the-air analog combiner of the signals radiated by the sensor nodes. The concurrent transmission of measurement data by different sensor nodes results in a superposition of signals ("channel collision") which can be exploited to compute a desired function over-the-air (such as the mean of the sensor measurements). Thereby, wireless data aggregation is achieved in the wave domain, simultaneously with wireless communication.

Besides such statistical and uncontrollable analog combining, deterministic and reconfigurable analog combining is of great importance in modern multi-element antenna systems – see Fig. 2. Proposals for reconfigurable analog combining already emerged in preparation of the 5G era, where beamforming with large-scale multi-element antenna arrays was envisioned but confronted with severe hardware complexity, cost, and energy consumption[52]. These issues arise when a complete RF chain is required for each antenna element. To overcome this limitation, hybrid analog/digital beamforming with a substantially reduced number of RF chains thanks to a reconfigurable analog combiner emerged. The analog combining was initially envisioned[22,53] and prototyped[54,55] in the form of circuits involving many phase shifters, or switches[56]. On the receive side, this analog combining circuit realizes a programmable linear mapping from the high-dimensional signal exiting the antenna ports to the low-dimensional signal entering the RF chains. A similar approach can be used in reverse order on the transmit side.

Meanwhile, efforts in microwave imaging were confronted with essentially the same challenge: to achieve the required resolution, large coherent apertures composed of many antenna elements are required – traditionally, with one RF chain per antenna

element. Here, the metamaterials platform has come to the rescue in three steps. *First*, static metasurfaces generating frequency-diverse pseudo-random scene illuminations were explored[25,57]. These implemented deterministic but static linear low-to-high-dimensional mappings; it was important to know the realized mapping and to ensure that it was pseudo-random (in line with compressed sensing principles), but there was no need to engineer one specific mapping. *Second*, dynamic metasurface antennas (DMAs) capable of generating sequences of pseudo-random scene illuminations based on random configurations enabled single-frequency operation[26,58,59]. The computational imaging principle was the same as in the frequency-diverse case. *Third*, the DMA's programmability was leveraged to optimize the analog combining end-to-end for a specific task, taking into account hardware impairments, task, prior scene knowledge, and measurement noise[27,60,61]. All versions of these computational microwave imagers can be understood as performing integrated sensing and wave-domain computing over the air; the latter is particularly advanced in the third case, where salient task-relevant information is already preselected in the wave domain.

DMAs integrate the reconfigurable analog combining into the antenna architecture so that they offer the wave-domain flexibility required for hybrid analog/digital beamforming in a more compact form-factor than the conventional use of separate analog combining circuits[23]. End-to-end optimization of DMAs for a specific task is also relevant in the context of wireless communications[62]. Besides DMAs, reconfigurable intelligent surfaces (RISs) have gained much traction in wireless communications research[39]. Conceptually, the key difference between RISs and DMAs is that DMAs have feeds so that they can radiate and/or receive waves in a programmable manner, whereas RISs do not have feeds so that they only scatter waves in a programmable manner. Use cases of RISs at the base station thus require separate feed antennas[63], and the programmable analog combining occurs partially over-the-air. This principle can also be generalized to hybrid transceivers leveraging stacked intelligent metasurfaces (SIMs)[24] instead of a conventional RIS. However, the main conceptually distinct use case for RISs in comparison to DMAs is the deployment of RISs away from the base station as programmable scatterers in a "smart" radio environment that can endow its wireless channels with desirable properties[64–67]. RISs thus offer a possibility to control the over-the-air analog combining in otherwise uncontrolled radio environments[21].

It is notable that existing examples of pWDC in the context of wireless systems are already integrated with sensing (in the case of computational imaging) or communications; in the future, further integration combining sensing, computing, and communications is expected. Overall, these schemes are necessarily hybrid, involving both wave-domain and digital steps. Thereby, they automatically resolve a concern about input/output overhead that exists for purely analog WDC. Indeed, it is important to address the question of how the input data is encoded into the impinging wavefront and how the output data is read out from the scattered wavefront. The associated input/output overhead can imply bottlenecks on speed, energy consumption, and/or footprint that may be difficult to amortize. In some cases, amortization is possible if the scale of the

implemented mathematical operation is sufficiently large to outweigh the input/output overhead. However, the input/output concern is altogether avoided in applications in which the input is naturally in the wave domain and the output is naturally in the digital domain; in such cases, there is no need for digital-to-analog conversion at the input, and the analog-to-digital conversion at the output is already present in any case. This is precisely the case for the existing examples of pWDC in the context of wireless systems.

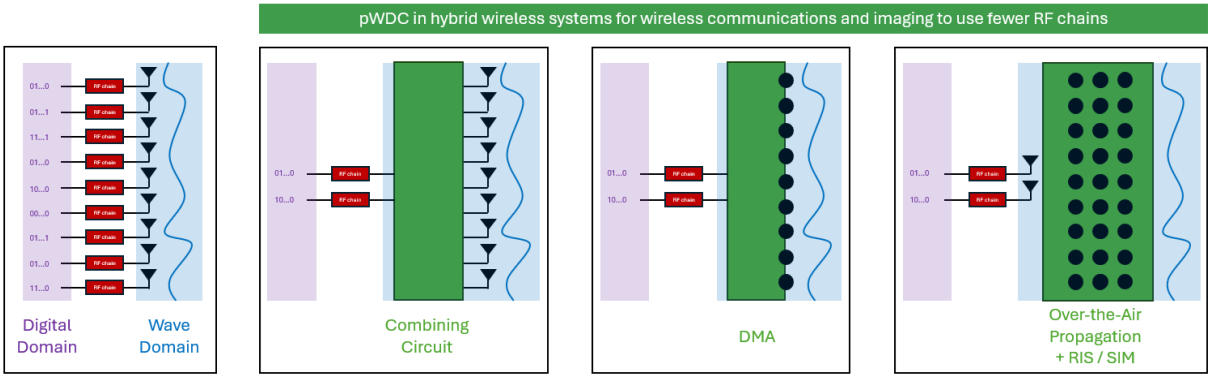

Figure 2: Selected examples of pWDC in hybrid wireless systems for MIMO wireless communications and computational imaging. *In all three cases, the goal is to use fewer RF chains by leveraging pWDC. Three major pWDC embodiments exist. Traditionally, a combining circuit between the RF chains and the antenna array is used. Most compactly, a dynamic metasurface antenna (DMA) compactly integrates everything. Alternatively, a RIS or SIM parametrizes over-the-air combination. The principle can be applied to transmission and reception.*

The fundamental ingredients of modern programmable metasurfaces like RISs and DMAs started to emerge since the early 2000s[34–36,68,3,37]. Typically, the reconfigurability mechanism relies on tunable lumped elements such as PIN diodes or varactor diodes. This common feature enables a universal approach to physics-compliant modeling of pWDC hardware that is described in BOX 1. Circuit-based pWDC hardware akin to analog combining circuits also continues to be explored[16,69] because it can be described with high accuracy using simplified closed-form models without accounting for mutual coupling. An ongoing quest in contemporary research relates to how to maximize the transfer-function tunability of pWDC hardware; an overview of four emerging concepts tackling this question is given in BOX 2.

BOX 1: Primer on physics-compliant modeling of pWDC hardware

For the vast majority of existing pWDC hardware for applications in wireless communications, the programmability relies on tunable lumped elements (for instance, PIN diodes or varactor diodes). At a high conceptual level, irrespective of the detailed architecture, all these pWDC hardware examples admit the same physics-consistent system model that rigorously captures all electromagnetically relevant coupling phenomena. The starting point is a partition of the system into three entities: (i) N_A ports via which waves can enter and exit the system; (ii) N_S tunable lumped elements; (iii) all other remaining system components (which are static by definition). Each tunable lumped element can be viewed as an additional "virtual" port terminated by a tunable load. Then, the overall N_A-port pWDC system can be viewed as the connection between a static (N_A+N_S)-port system and a tunable N_S-port system. Each constituent system is characterized by a scattering matrix; the scattering matrix is diagonal for the tunable system, given its composition of tunable individual loads. The scattering coefficients describing the static constituent system are generally not known in closed form because they account for environmental and structural scattering. They must generally be extracted from a full-wave simulation or be estimated experimentally – see Sec. 3.

The complexity of the static structural and environmental scattering is immaterial to the applicability of this multiport network system model and its number of parameters (which depends only on the number of actual and "virtual" ports). The described model even applies to "beyond-diagonal" programmable metasurfaces (see BOX 2) when their implementation relies on tunable lumped elements[70,71]. An illustration of this model for a complex RIS-parametrized rich-scattering environment is shown below, together with the corresponding equation for evaluating the connection of the two constituent subsystems. Upon inspection of the equation, it is apparent that the mapping from the PM's load vector to the resulting transfer function is generally non-linear due to the matrix inversion. Physically, this makes sense because of the coupling effects between the tunable elements. This can be seen more clearly by rewriting the matrix inversion as an infinite sum, in which the kth term corresponds to the family of all k-bounce paths. Paths bouncing off multiple tunable elements inevitably intertwine the impact of the tunable elements on the transfer function. The coupling-induced non-linear mapping from configuration to transfer function complicates optimization but enables enhanced wave-domain flexibility (see BOX 2) and the implementation of non-linear functions (see Sec. 4). In addition, the encoding function mapping the PM's control vector to the PM's load vector is generally non-linear and thus another resource for implementing non-linear functions (see Sec. 4). The encoding function is outside the wave domain.

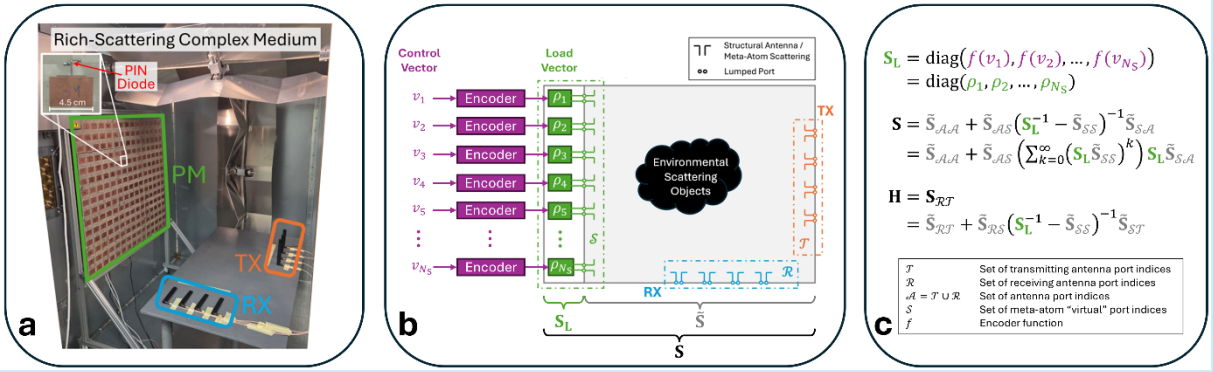

Figure 3: Universal physics-compliant system model applied to a rich-scattering multiple-input multiple-output system parametrized by a large programmable metasurface (PM). *The system is illustrated with a photographic image in (a), the corresponding multiport-network schematic is shown in (b), and the associated equations are summarized in (c). The equation maps a control vector $(v_1, v_2, \ldots, v_{N_S})$ via an encoding function $\rho_i = f(v_i)$ to the PM's load vector $(\rho_1, \rho_2, \ldots, \rho_{N_S})$. The latter determines the PM's load matrix $\boldsymbol{S_L}$ which is mapped to the measurable scattering matrix $\boldsymbol{S}$ via multiport network theory. The involved matrix inversion can be recast as an infinite sum of matrix powers, where the kth term represents the family of all k-bounce paths. The wireless channel matrix $\boldsymbol{H}$ is an off-diagonal block of $\boldsymbol{S}$. The number of model parameters does not depend on the complexity of the scattering, being fixed solely by the number of antennas and programmable meta-atoms.*

BOX 2: Four emerging concepts for maximizing wave-domain flexibility

Given the pivotal role of wave-domain programmability for adapting to dynamic use cases, time-multiplexed multi-functionality, and robustness to fabrication inaccuracies, it is pivotal to understand how to design pWDC hardware with maximally flexible wave-domain properties. Four distinct and complementary answers to this question emerge in the literature. Their relevance to a specific application depends on the latter's constraints (for instance, regarding footprint, thickness, number of tunable components, control circuit complexity, spectrum allotment).

First, because the wavefront transformations that can be realized with a single linear metasurface layer are often limited, there are several proposals for **stacking multiple metasurfaces** to achieve enhanced wave control[5–10,45,72]. Common wave-control goals include maximizing the normalized fidelity with which a target transformation is approximated and the power throughput into the intended output subspace ("output diffraction efficiency"). More layers generally increase the degrees of freedom and thereby the ability to improve both fidelity and efficiency; yet, even with a fixed number of degrees of freedom, multi-layer structures can outperform shallower structures in which uncontrolled ballistic photons limit the achievable fidelity.[72] Recent stacked intelligent metasurfaces (SIMs) combine the idea of stacking with programmability[10,24]. These approaches achieve higher transfer-function flexibility typically at the expense of a less compact system and requiring more tunable components. In the absence of non-linearities, the overall transformation realized by a stack of metasurfaces is linear and can be represented by a single matrix. The benefits of the stack over a single layer relate to the achieved fidelity, tunability, and/or efficiency.

Second, beyond locally tuning the meta-atoms in a programmable metasurface (such as an RIS or a DMA), there are proposals for additionally **tuning the non-local interactions** between meta-atoms[40,73,74,70]. These approaches achieve higher transfer-function tunability at the expense of requiring more tunable components. Envisioned beyond-diagonal programmable metasurfaces can be partitioned into a static antenna structure, static components of a load circuit, and tunable lumped elements[71]. In such embodiments, the programmability is point-like (lumped), and in that sense local[71] – but the tunable components are not in one-to-one correspondence with the meta-atoms. Regardless of the terminology, the increased number of tunable elements improves the wave-domain flexibility compared to conventional programmable metasurfaces.

Third, there is increasing evidence that **stronger mutual coupling** between the tunable elements increases the transfer-function tunability[75–78]. The intuitive reason is that the wave bounces more often between the tunable components, allowing it to accumulate more sensitivity to their configuration[75]. These approaches achieve higher transfer-function flexibility at the expense of a stronger non-linearity in the forward mapping from configuration to transfer function (which can be reaped as a benefit, see Sec. 4), and a stronger vulnerability to perturbations.

Fourth, beyond quasi-static programmable metasurfaces whose properties are reconfigurable but static during a given measurement, **time modulation** offers additional degrees of freedom that are leveraged by space-time-coding (STC) programmable metasurfaces[79]. Neglecting mutual coupling, the STC concept has recently been explored for RISs[79–81] and DMAs[82]. A mutual-coupling-aware STC system model was also proposed[83], but it remains unexplored whether the aforementioned insights about the influence of the strength and tunability of mutual coupling on the transfer-function tunability carry over to STC approaches. Altogether, STC approaches achieve higher transfer-function flexibility at the expense of a more complex control circuitry and potential sideband pollution.

3. Prototype-aware optimization for pWDC

A pressing practical challenge for pWDC lies in determining how to configure the programmable wave system during runtime so that its transfer function approximates the desired one as closely as possible. Theoretically, the underlying high-dimensional, non-convex, non-linear optimization problems are challenging but well studied. Such theoretically studied approaches can be classified as centralized in-silico optimization: a central operator with perfect system knowledge utilizes a traditional digital computer to optimize the system configuration.

The experimentally achieved performance of centralized in-silico optimization hinges on the accuracy of the utilized system model. Model-reality mismatch can originate from the model architecture (for instance, when fundamental physical phenomena such as mutual coupling are neglected) or the choice of model parameters (for instance, when fabrication inaccuracies result in deviations from the assumed properties). If model-reality mismatch is inevitable, one can explicitly account for uncertainties by including suitable random variables in the system model. This approach has been shown to achieve robustness to misalignment in cascaded diffractive multi-layer structures[84,85], but this robustness inevitably comes at the expense of performance degradations that scale with the range of the accounted uncertainties. Moreover, strategies to boost wave-domain flexibility based on strong mutual coupling (see BOX 2) are fundamentally more sensitive to inaccuracies and risk being counter-productive without an accurate system model. In many cases, it is thus crucial to minimize any mismatch between the model and the experimentally given prototype.

A useful taxonomy considers the model's architecture and the origin of its parameter values. The model architecture can be purely physics-based (such as the multiport network model described in BOX 1), fully physics-agnostic (such as a feed-forward neural network), or a combination of both[86]. It is generally favorable to incorporate as much physics knowledge as possible into the architecture to endow the model with a physics-based inductive bias. The model parameters can be estimated numerically (based on the assumed system details) or experimentally. For pWDC hardware leveraging tunable lumped elements (for instance, PIN diodes or varactor diodes) to achieve reconfigurability, a universal physics-consistent system model exists (see BOX 1). Assuming perfect system knowledge, the model parameters can be obtained with a single numerical simulation[87,88]. However, perfect system knowledge is rare, and the required simulation can be computationally costly. Thus, an experimental estimation of the model parameters is usually needed[89,90]. This experimental parameter estimation is subject to inevitable ambiguities, but they are operationally irrelevant for system optimization[90]. For typical pWDC hardware such as RISs and DMAs with a few hundred tunable components, compact physical-model calibration and efficient model-based optimization (leveraging tricks like the Woodbury identity for efficiently updating previous forward evaluations[91]) is a viable and promising approach.

For larger-scale pWDC systems, model-based optimization can become unfeasible. Inspiring ideas for possible model-agnostic techniques are proposed in recent literature on training physical neural networks (PNNs)[92]. Zeroth-order methods, such as a simple coordinate descent, avoid the need for a model but scale poorly with the number of model parameters. Advanced model-agnostic methods like in-situ reinforcement learning can reduce the number of required measurements[93,94]. One elegant alternative model-agnostic idea consists of physically implementing the backpropagation algorithm that underpins the training of digital neural networks[95,96]. However, this requires additional hardware to inject coherent wavefronts via the PNN's output ports and intensity detectors at each tunable component. Another potential solution is to eliminate the need for gradients altogether by using physical local learning[19,97], where each layer is configured based on two forward passes, one with positive data and one with negative data. However, the performance in large-scale PNNs remains unexplored.

As summarized in Fig. 4, all thus-far discussed optimization techniques rely on a central operator. Incidentally, this operator is an abstract concept, not limited to a human but also applicable to human-written code[98] and groups of artificial-intelligence agents acting as operators[99]. In any case, the reliance on a central operator likely imposes fundamental limits on scalability due to communications overhead between the operator and the tunable components. This raises the following question: can pWDC hardware self-configure in a decentralized manner? While a concept for a decentralized self-configuring linear circuit exists[100], it is specific to one particular, feed-forward-only circuit architecture and is not applicable to generic pWDC hardware. Identifying analogous concepts for generic pWDC would constitute a major advance, but it is unclear whether that is even possible without fundamentally requiring non-linear mechanisms, such as harmonic feedback[101] or self-oscillation[102].

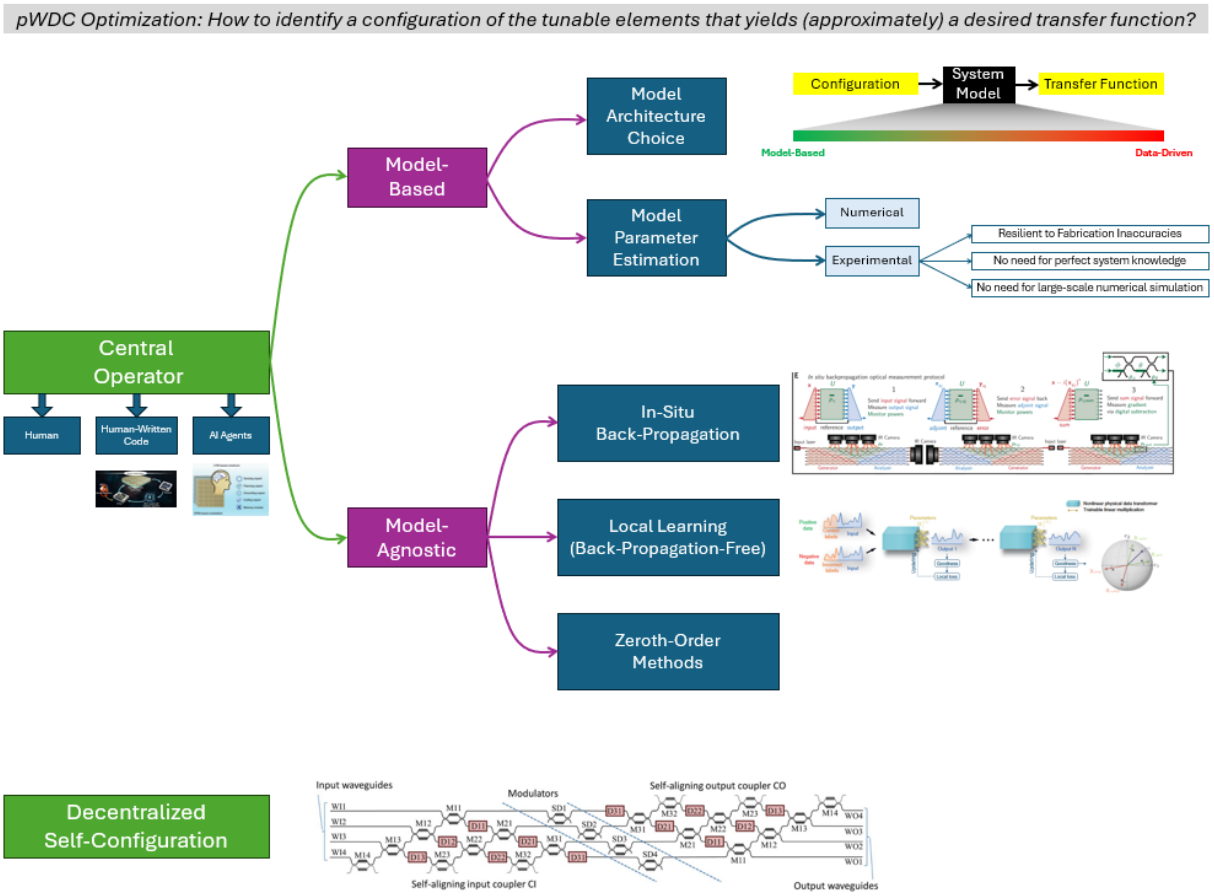

Figure 4: Taxonomy of approaches to prototype-aware pWDC optimization. *Existing schemes for optimizing experimental pWDC hardware rely on a central operator, which can be a human, a human-written code[98], or a group of AI agents[99]. The central operator optimizes the pWDC hardware either in a model-based or model-agnostic manner. In the former case, a model architecture is chosen somewhere on the spectrum between purely physics-based and fully data-driven (physics-agnostic), and the model parameters are estimated, either numerically or experimentally. In model-agnostic optimization, interesting alternatives to poorly scaling zeroth-order methods include in-situ back-propagation[96] and back-propagation-free local learning[19]. Decentralized self-configuration of pWDC hardware is extremely rare to date, and has only been explored for special architectures of Mach-Zehnder-interferometer meshes[100].*

4. Beyond linear continuous-wave pWDC

While pWDC hardware for reconfigurable linear transformations of continuous-wave operations is already quite mature at the prototype level, it is of great interest to expand the scope of realizable wave-domain operations[103].

The most obvious concern regards non-linearity. Non-linearities are indispensable in many advanced signal-processing algorithms. They are the essential ingredient for the universal approximation theorem for digital neural networks[104]. As shown in Fig. 5, implementations of nonlinear RF wave-domain processing are in principle possible using all-RF nonlinear circuit components, such as strongly driven limiters or saturating amplifiers. However, these RF nonlinearities are typically engineered to operate at comparatively high RF power levels, which are usually incompatible with the signal levels and energy budget targeted in pWDC systems. Meanwhile, implementing non-linear transformations outside the wave domain (e.g., in analog electronics or digital processing) is easier. Most proposals for non-linear pWDC are thus inherently hybrids between the wave domain and the analog-electronics or digital domain. In hybrid architectures, read-out non-linearities arising from bare intensity detection are readily available[10] but not sufficiently strong for implementing advanced non-linear operations. Non-linearities such as one resembling the common ReLU activation function can be implemented in analog electronics by driving a tunable gain element with a DC output signal from an RF detector, with latencies of tens of nanoseconds[105]. More elaborate non-linearities can be implemented in the digital domain at the expense of longer latencies. For instance, some schemes integrate linear pWDC hardware into a hybrid pipeline together with a non-linear digital backend (such as a digital artificial neural network) for end-to-end optimized integrated over-the-air computing and sensing[27], circuital non-linear feedback architectures[69], or feedback-loop-based architectures for inverse design[16]. This approach can be extended to enable neuromorphic realizations of wave-domain PNNs, for instance, with hidden spiking layers. The hybrid nature of such schemes can be a significant caveat if it implies additional analog-to-digital and digital-to-analog conversions, which constitute speed bottlenecks and dominate power consumption.

Another route toward non-linearity consists in tuning structural parameters of the system as a function of the input data – see Fig. 5. While the mapping from input wavefront to output wavefront is by definition linear in a reconfigurable linear wave system, the mapping from configuration to transfer function (or output wavefront for a reference input wavefront) is generally non-linear. BOX 1 explains the two reasons: *first*, the encoding function generally constitutes a non-linear mapping from control vector to structural parameters (load vector), and, *second*, mutual coupling between the tunable elements causes a non-linear mapping from structural parameters (load vector) to transfer function. These two effects, also referred to as “encoding non-linearity” and “structural non-linearity”, enable the realization of a non-linear mapping at the system level, despite linear wave propagation for any fixed configuration. Neither of the two effects is a pure

wave-domain non-linearity: an encoding non-linearity occurs outside the wave domain; a structural non-linearity, while occurring in the wave domain, requires encoding of input data into structural parameters. Incidentally, encoding input data into the structural system parameters (as opposed to the input wavefront) is the basis of backscatter communications, whose principle dates back at least to the Great Seal Bug[106] from the 1940s and is nowadays omnipresent in RFID technology.

Examples of encoding non-linearities include amplitude, intensity and phase encoding[107], the latter of which has been shown in the context of diffractive multi-layer structures to enable highly expressive approximations of desired nonlinear functions[33]. Quantization of the structural parameters' tunability usually results in an inevitable encoding non-linearity, unless the input data is already discrete on a compatible alphabet. For the special case of binary input data and 1-bit-programmable structural parameters, which is common for programmable metasurface prototypes, the encoding function is always affine (linear plus a constant term).

As for structural nonlinearity, the non-linear mapping from programmable-metasurface configuration to transfer function inside a rich-scattering cavity was explicitly noted in Ref.[17], where it was deliberately mitigated to implement a linear operation. An analogous optical system was realized in Ref.[29]. A more involved version of structural non-linearity was theoretically studied for a time-varying system in Ref.[28]. Experimental demonstrations of structural non-linearity in PNNs were initially reported for microwaves[19] and subsequently also transposed to optics[30,32]. Structural non-linearity arises because of a superposition of multi-bounce paths that interact multiple times with the input-data-carrying structural parameters ("virtual data repetition"). The precise mathematical form of structural non-linearity relates to a matrix inversion which compactly sums the contributions of all multi-bounce paths, as seen in Fig. 3c. By judiciously mapping input data to structural parameters, one can thus realize matrix-inversion-type operations such as those underpinning linear minimum mean square error estimation[108]. A related but distinct implementation of structural non-linearity in Ref.[31] unfolds the repeated interactions into a forward-multiple-scattering cascade of sequential programmable modulation planes into which the same input data is encoded. Because structural non-linearity requires by construction the (usually non-linear) encoding of input data into structural parameters, it is accompanied by an encoding non-linearity in most implementations.

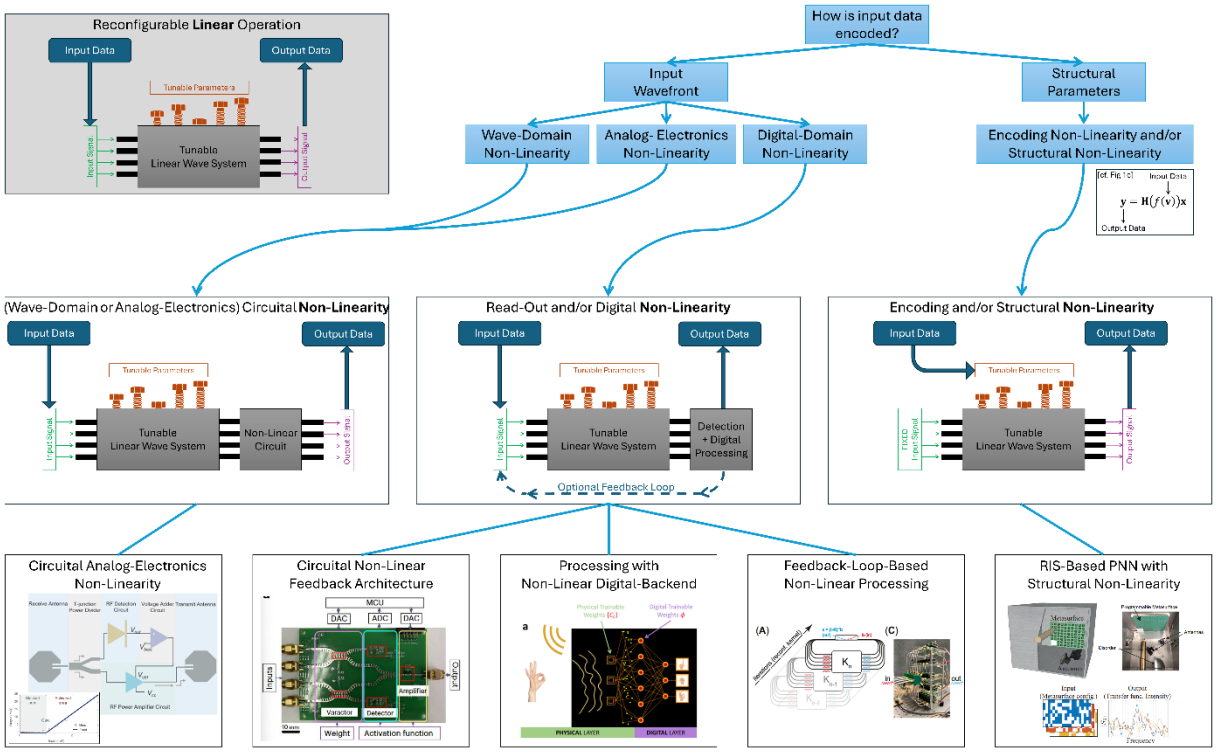

Figure 5: Routes toward non-linear processing with pWDC hardware. *Taxonomy (top row), corresponding schematics (middle row) and selected examples[105,69,27,16,19] of experimental implementations of non-linear operations leveraging pWDC hardware.*

Besides non-linearity, memory is often an important feature in advanced signal processing algorithms. Within the realm of linear time-invariant wave systems, systems with long dwell times exhibit a form of fading memory. For example, a static integrated photonic chaotic cavity has been demonstrated to have a memory of up to 6 bits, which is useful for header recognition in telecom applications[109]. Interestingly, long dwell times also tend to lead to strong mutual coupling between the tunable components, which improves the transfer-function flexibility, as discussed in BOX 2. Beyond the scope of time-invariant systems, switched networks can exceed the delay-bandwidth limit[110], offering another potential route to a form of memory.

Ultimately, the limiting factor regarding beyond-linear continuous-wave pWDC is not only the hardware realization but also the identification of a compelling use case in which the additional cost (for instance, regarding latency or power consumption) can be amortized. Simple linear continuous-wave pWDC, possibly augmented by a digital backend performing non-linear operations, is poised for initial deployments, while the compatibility with a convincing use case is an important concern for more complex pWDC hardware proposals.

5. Integrating pWDC into system-level architectures

Integrating pWDC into wireless networks requires concerted efforts across layers, ranging from the technology and device layers via the application layer to the overall network architecture design. pWDC constitutes a fundamentally new type of resource that must be appropriately managed so that it can be seamlessly integrated into the overall network architecture. To date, most research efforts have focused on the technology and device layers (for instance, how to design an RIS or a DMA and what technology maximizes its wave-domain flexibility) and have demonstrated their suitability for selected applications (for instance, beam-forming, computational imaging, or direction-of-arrival estimation). However, a holistic network-level view, abstracting pWDC as a shared, schedulable resource rather than a micromanaged device, is still largely missing. Applying common virtualization techniques to pWDC resources in the spirit of network slicing (sharing a physical resource among multiple applications[111], see Fig. 6) may fundamentally struggle with electromagnetic phenomena occurring at the device level. For instance, coupling and interference phenomena between distinct pWDC hardware slices can undermine the intended functioning.

Integrating pWDC into system-level architectures calls for an operating-system (OS) view in which pWDC is treated as a shared, schedulable resource[112]. As shown in Fig. 6, this OS layer is interposed between applications and the heterogeneous pWDC hardware. Within the OS, a service broker lets ordinary applications ask for connectivity, sensing, security or wireless power without naming specific hardware; an orchestrator translates those demands into plans, possibly consulting a simulator to anticipate how nearby pWDC hardware will interact, and then uses a scheduler to multiplex tasks across time, frequency and space; beneath it, a hardware manager hides heterogeneity and pushes pre-validated configurations to both existing and newly deployed pWDC hardware while drawing on sensors, access points and base stations for feedback. Given the rapid advances in artificial intelligence (AI), AI-based workflow automation is becoming increasingly feasible and likely. Workflow automation in a prototypical smart radio environment based on a group of AI agents, each with dedicated expertise (such as a hardware manager or scheduler) and communicating in natural language, was recently prototyped[99]. These early tests, displayed in Fig. 6, already tackled moderately complex scenarios involving RIS resources to facilitate a combination of sensing and communications objectives as part of a sequence of self-defined tasks.

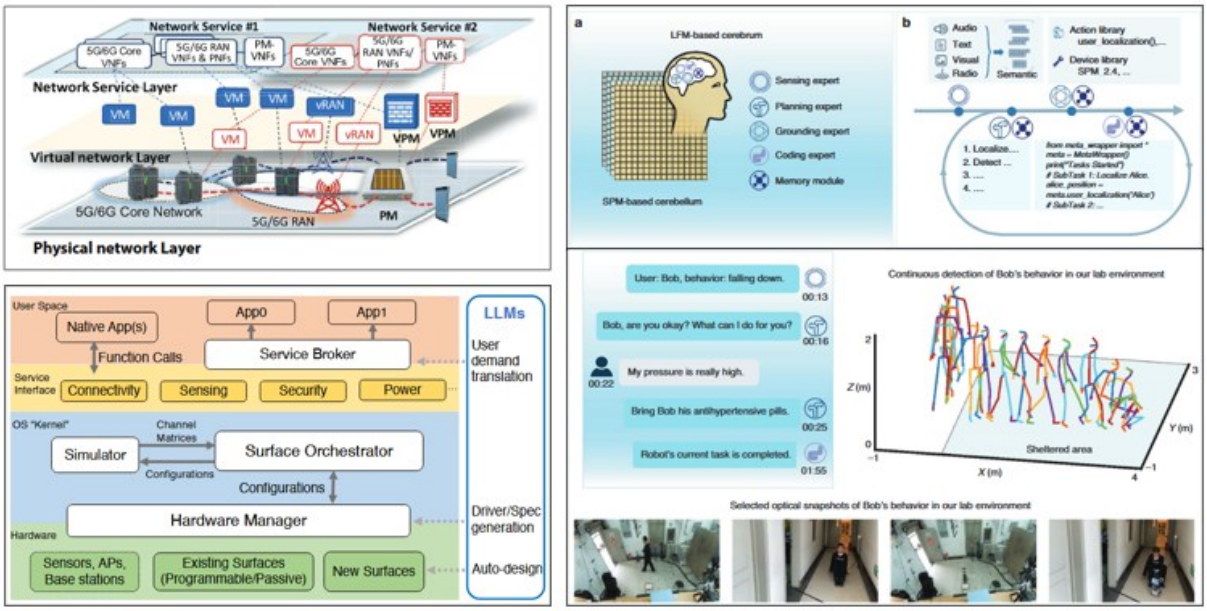

Figure 6: AI-driven pWDC resource management at the network level. *(top left) Virtualization concept for sharing pWDC hardware (here RIS) among different network services.[111] (bottom left) Overview of a possible ecosystem in which an operating system manages pWDC hardware, possibly with AI-based workflow automation[112]. (right) Prototype of a group of AI agents, each with distinct expertise and communicating in natural language, that autonomously plan and execute a complex sequence of self-defined tasks, leveraging pWDC hardware (here RIS) for wireless sensing and communications[99].*

6. Discussion

The last two decades have witnessed rapid progress in developing hardware and exploring applications for pWDC across wave phenomena, including the microwave regime that is currently most relevant to wireless communications. Programmable metasurfaces unlock advanced wave control that endows wave-domain signal processing with unprecedented flexibility. Hybrid systems combining pWDC with digital processing are already among the most prominent systems considered for pWDC-empowered wireless sensing and communications. Because hybrid systems can avoid the additional overhead and cost that would arise from extra conversions between analog and digital domains, as well as synergistically combine the distinct advantages of each domain, they are poised to be one of the most promising directions for transitioning pWDC to real-life applications in the wireless domain.

Encouraged by recent prototype systems at the device and application levels, important questions for future research span from fundamental aspects to the system-level architecture. Perhaps most fundamentally, theoretical tools for understanding the expressivity of pWDC are missing; electromagnetically consistent bounds on transfer functions that can be realized with a given pWDC hardware remain unknown to date. Understanding the range of realizable mathematical operations gets even more complicated as we go beyond linear continuous-wave systems. At the same time, the trade-offs between hardware complexity and performance gains are unexplored. For instance, are the latency and power consumption penalties of implementing non-linear pWDC worth the ensuing benefits? Mapping out the complexity-performance Pareto frontier is an important avenue for future work, with the notion of complexity encompassing both the complexity of realizing the hardware as well as the complexity of the necessary efforts to optimize the hardware configuration in real time.

In addition, several practical aspects, such as footprint, power consumption, and security, have not been the center of recent research on pWDC. For instance, the marked differences in compactness among the three hybrid antenna architecture families in Fig. 2 have not received much attention. Given the potential of metamaterial engineering to miniaturize devices and maximize their wave-domain flexibility with a fixed budget of tunable components, there remain important avenues for metamaterials research on the technology level. At the same time, reliable end-to-end evaluations of power budgets are urgently needed. Finally, we anticipate that security considerations, both on the physical layer and in AI-empowered operating systems for pWDC, will become increasingly important.

7. References

1. McMahon, P. L. The physics of optical computing. *Nat. Rev. Phys.* **5**, 717–734 (2023).
2. Zangeneh-Nejad, F., Sounas, D. L., Alù, A. & Fleury, R. Analogue computing with metamaterials. *Nat. Rev. Mater.* **6**, 207–225 (2021).
3. Cui, T. J., Qi, M. Q., Wan, X., Zhao, J. & Cheng, Q. Coding metamaterials, digital metamaterials and programmable metamaterials. *Light Sci. Appl.* **3**, e218–e218 (2014).
4. Reck, M., Zeilinger, A., Bernstein, H. J. & Bertani, P. Experimental realization of any discrete unitary operator. *Phys. Rev. Lett.* **73**, 58–61 (1994).
5. Morizur, J.-F. *et al.* Programmable unitary spatial mode manipulation. *J. Opt. Soc. Am. A* **27**, 2524 (2010).
6. Berkhout, G. C. G., Lavery, M. P. J., Courtial, J., Beijersbergen, M. W. & Padgett, M. J. Efficient Sorting of Orbital Angular Momentum States of Light. *Phys. Rev. Lett.* **105**, 153601 (2010).
7. Pfeiffer, C. & Grbic, A. Cascaded metasurfaces for complete phase and polarization control. *Applied Physics Letters* **102**, 231116 (2013).
8. Lin, X. *et al.* All-optical machine learning using diffractive deep neural networks. *Science* **361**, 1004–1008 (2018).
9. Zhou, T. *et al.* Large-scale neuromorphic optoelectronic computing with a reconfigurable diffractive processing unit. *Nat. Photonics* **15**, 367–373 (2021).
10. Liu, C. *et al.* A programmable diffractive deep neural network based on a digital-coding metasurface array. *Nat. Electron.* **5**, 113–122 (2022).
11. Dong, J., Rafayelyan, M., Krzakala, F. & Gigan, S. Optical Reservoir Computing Using Multiple Light Scattering for Chaotic Systems Prediction. *IEEE J. Select. Topics Quantum Electron.* **26**, 1–12 (2020).
12. Matthès, M. W., del Hougne, P., de Rosny, J., Lerosey, G. & Popoff, S. M. Optical complex media as universal reconfigurable linear operators. *Optica* **6**, 465 (2019).
13. Silva, A. *et al.* Performing Mathematical Operations with Metamaterials. *Science* **343**, 160–163 (2014).
14. Mohammadi Estakhri, N., Edwards, B. & Engheta, N. Inverse-designed metastructures that solve equations. *Science* **363**, 1333–1338 (2019).
15. Esfahani, S., Cotrufo, M. & Alù, A. Tailoring Space-Time Nonlocality for Event-Based Image Processing Metasurfaces. *Phys. Rev. Lett.* **133**, 063801 (2024).
16. Tzarouchis, D. C., Edwards, B. & Engheta, N. Programmable wave-based analog computing machine: a metastructure that designs metastructures. *Nat. Commun.* **16**, 908 (2025).
17. del Hougne, P. & Lerosey, G. Leveraging Chaos for Wave-Based Analog Computation: Demonstration with Indoor Wireless Communication Signals. *Phys. Rev. X* **8**, 041037 (2018).

18. Sol, J., Smith, D. R. & del Hougne, P. Meta-programmable analog differentiator. *Nat. Commun.* **13**, 1713 (2022).
19. Momeni, A., Rahmani, B., Malléjac, M., del Hougne, P. & Fleury, R. Backpropagation-free training of deep physical neural networks. *Science* **382**, 1297–1303 (2023).
20. Giridhar, A. & Kumar, P. R. Computing and communicating functions over sensor networks. *IEEE J. Select. Areas Commun.* **23**, 755–764 (2005).
21. Garcia Sanchez, S. *et al.* AirNN: Over-the-Air Computation for Neural Networks via Reconfigurable Intelligent Surfaces. *IEEE/ACM Trans. Networking* **31**, 2470–2482 (2023).
22. Zhang, X., Molisch, A. F. & Kung, S.-Y. Variable-phase-shift-based RF-baseband codesign for MIMO antenna selection. *IEEE Trans. Signal Process.* **53**, 4091–4103 (2005).
23. Shlezinger, N., Alexandropoulos, G. C., Imani, M. F., Eldar, Y. C. & Smith, D. R. Dynamic Metasurface Antennas for 6G Extreme Massive MIMO Communications. *IEEE Wirel. Commun.* **28**, 106–113 (2021).
24. An, J. *et al.* Stacked Intelligent Metasurface-Aided MIMO Transceiver Design. *IEEE Wirel. Commun.* **31**, 123–131 (2024).
25. Hunt, J. *et al.* Metamaterial Apertures for Computational Imaging. *Science* **339**, 310–313 (2013).
26. Sleasman, T., F. Imani, M., Gollub, J. N. & Smith, D. R. Dynamic metamaterial aperture for microwave imaging. *Appl. Phys. Lett.* **107**, 204104 (2015).
27. del Hougne, P., Imani, M. F., Diebold, A. V., Horstmeyer, R. & Smith, D. R. Learned Integrated Sensing Pipeline: Reconfigurable Metasurface Transceivers as Trainable Physical Layer in an Artificial Neural Network. *Adv. Sci.* **7**, 1901913 (2019).
28. Momeni, A. & Fleury, R. Electromagnetic wave-based extreme deep learning with nonlinear time-Floquet entanglement. *Nat. Commun.* **13**, 2651 (2022).
29. Eliezer, Y., Rührmair, U., Wisiol, N., Bittner, S. & Cao, H. Tunable nonlinear optical mapping in a multiple-scattering cavity. *Proc. Natl. Acad. Sci. U.S.A.* **120**, e2305027120 (2023).
30. Xia, F. *et al.* Nonlinear optical encoding enabled by recurrent linear scattering. *Nat. Photonics* **18**, 1067–1075 (2024).
31. Yildirim, M., Dinc, N. U., Oguz, I., Psaltis, D. & Moser, C. Nonlinear processing with linear optics. *Nat. Photonics* **18**, 1076–1082 (2024).
32. Wanjura, C. C. & Marquardt, F. Fully nonlinear neuromorphic computing with linear wave scattering. *Nat. Phys.* **20**, 1434–1440 (2024).
33. Rahman, M. S. S., Li, Y., Yang, X., Chen, S. & Ozcan, A. Massively parallel and universal approximation of nonlinear functions using diffractive processors. *eLight* **5**, 32 (2025).
34. Sievenpiper, D. *et al.* A tunable impedance surface performing as a reconfigurable beam steering reflector. *IEEE Trans. Antennas Propag.* **50**, 384–390 (2002).

35. Kamoda, H., Iwasaki, T., Tsumochi, J., Kuki, T. & Hashimoto, O. 60-GHz Electronically Reconfigurable Large Reflectarray Using Single-Bit Phase Shifters. *IEEE Trans. Antennas Propagat.* **59**, 2524–2531 (2011).
36. Clemente, A., Dussopt, L., Sauleau, R., Potier, P. & Pouliguen, P. 1-Bit Reconfigurable Unit Cell Based on PIN Diodes for Transmit-Array Applications in X-Band. *IEEE Trans. Antennas Propagat.* **60**, 2260–2269 (2012).
37. Kaina, N., Dupré, M., Fink, M. & Lerosey, G. Hybridized resonances to design tunable binary phase metasurface unit cells. *Opt. Express* **22**, 18881 (2014).
38. Liaskos, C. *et al.* A New Wireless Communication Paradigm through Software-Controlled Metasurfaces. *IEEE Commun. Mag.* **56**, 162–169 (2018).
39. Basar, E. *et al.* Wireless Communications Through Reconfigurable Intelligent Surfaces. *IEEE Access* **7**, 116753–116773 (2019).
40. Shen, S., Clerckx, B. & Murch, R. Modeling and Architecture Design of Reconfigurable Intelligent Surfaces Using Scattering Parameter Network Analysis. *IEEE Trans. Wirel. Commun.* **21**, 1229–1243 (2022).
41. An, J. *et al.* Stacked Intelligent Metasurfaces for Efficient Holographic MIMO Communications in 6G. *IEEE J. Select. Areas Commun.* **41**, 2380–2396 (2023).
42. Goodman, J. W., Dias, A. R. & Woody, L. M. Fully parallel, high-speed incoherent optical method for performing discrete Fourier transforms. *Opt. Lett.* **2**, 1 (1978).
43. Sanghadasa, M., Erbach, P. S., Sung, C. C., Gregory, D. A. & Friday, W. A. Application of wavelet transform to synthetic aperture radar and its optical implementation. in (ed. Szu, H. H.) 346 (Orlando, FL, 1994). doi:10.1117/12.170038.
44. Kwon, H., Sounas, D., Cordaro, A., Polman, A. & Alù, A. Nonlocal Metasurfaces for Optical Signal Processing. *Phys. Rev. Lett.* **121**, 173004 (2018).
45. Kulce, O., Mengu, D., Rivenson, Y. & Ozcan, A. All-optical synthesis of an arbitrary linear transformation using diffractive surfaces. *Light Sci. Appl.* **10**, 196 (2021).
46. Shen, Y. *et al.* Deep learning with coherent nanophotonic circuits. *Nat. Photonics* **11**, 441–446 (2017).
47. Bogaerts, W. *et al.* Programmable photonic circuits. *Nature* **586**, 207–216 (2020).
48. Nikkhah, V. *et al.* Inverse-designed low-index-contrast structures on a silicon photonics platform for vector–matrix multiplication. *Nat. Photon.* **18**, 501–508 (2024).
49. Nazer, B. & Gastpar, M. Computation Over Multiple-Access Channels. *IEEE Trans. Inform. Theory* **53**, 3498–3516 (2007).
50. Goldenbaum, M., Boche, H. & Stanczak, S. Harnessing Interference for Analog Function Computation in Wireless Sensor Networks. *IEEE Trans. Signal Process.* **61**, 4893–4906 (2013).
51. Goldenbaum, M. & Stanczak, S. Robust Analog Function Computation via Wireless Multiple-Access Channels. *IEEE Trans. Commun.* **61**, 3863–3877 (2013).

52. Han, S., I, C., Xu, Z. & Rowell, C. Large-scale antenna systems with hybrid analog and digital beamforming for millimeter wave 5G. *IEEE Commun. Mag.* **53**, 186–194 (2015).
53. Venkateswaran, V. & Van Der Veen, A.-J. Analog Beamforming in MIMO Communications With Phase Shift Networks and Online Channel Estimation. *IEEE Trans. Signal Process.* **58**, 4131–4143 (2010).
54. Roh, W. *et al.* Millimeter-wave beamforming as an enabling technology for 5G cellular communications: theoretical feasibility and prototype results. *IEEE Commun. Mag.* **52**, 106–113 (2014).
55. Gong, T. *et al.* RF Chain Reduction for MIMO Systems: A Hardware Prototype. *IEEE Syst. J.* **14**, 5296–5307 (2020).
56. Mendez-Rial, R., Rusu, C., Gonzalez-Prelcic, N., Alkhateeb, A. & Heath, R. W. Hybrid MIMO Architectures for Millimeter Wave Communications: Phase Shifters or Switches? *IEEE Access* **4**, 247–267 (2016).
57. Gollub, J. N. *et al.* Large Metasurface Aperture for Millimeter Wave Computational Imaging at the Human-Scale. *Sci. Rep.* **7**, 42650 (2017).
58. Wang, L., Li, L., Li, Y., Zhang, H. C. & Cui, T. J. Single-shot and single-sensor high/super-resolution microwave imaging based on metasurface. *Sci. Rep.* **6**, 26959 (2016).
59. Sleasman, T. *et al.* Implementation and characterization of a two-dimensional printed circuit dynamic metasurface aperture for computational microwave imaging. *IEEE Trans. Antennas Propag.* **69**, 2151 (2020).
60. Li, H.-Y. *et al.* Intelligent Electromagnetic Sensing with Learnable Data Acquisition and Processing. *Patterns* **1**, 100006 (2020).
61. Qian, C. & del Hougne, P. Noise-Adaptive Intelligent Programmable Meta-Imager. *Intell. Comput.* **2022**, 2022/9825738 (2022).
62. Wang, H. *et al.* Dynamic Metasurface Antennas for MIMO-OFDM Receivers With Bit-Limited ADCs. *IEEE Trans. Commun.* **69**, 2643–2659 (2021).
63. Huang, Y., Zhu, L. & Zhang, R. Integrating Base Station with Intelligent Surface for 6G Wireless Networks: Architectures, Design Issues, and Future Directions. *IEEE Wireless Commun.* 1–8 (2025) doi:10.1109/MWC.010.2400211.
64. Subrt, L. & Pechac, P. Intelligent walls as autonomous parts of smart indoor environments. *IET Commun.* **6**, 1004 (2012).
65. del Hougne, P., Fink, M. & Lerosey, G. Optimally diverse communication channels in disordered environments with tuned randomness. *Nat. Electron.* **2**, 36–41 (2019).
66. Li, Z. *et al.* Towards Programming the Radio Environment with Large Arrays of Inexpensive Antennas. *Proc. USENIX NSDI* 285–300 (2019).
67. Di Renzo, M. *et al.* Smart Radio Environments Empowered by Reconfigurable Intelligent Surfaces: How It Works, State of Research, and The Road Ahead. *IEEE J. Select. Areas Commun.* **38**, 2450–2525 (2020).

68. Venneri, F., Costanzo, S. & Di Massa, G. Design and Validation of a Reconfigurable Single Varactor-Tuned Reflectarray. *IEEE Trans. Antennas Propagat.* **61**, 635–645 (2013).
69. Gao, X. *et al.* Programmable surface plasmonic neural networks for microwave detection and processing. *Nat. Electron.* **6**, 319–328 (2023).
70. Prod'homme, H. & del Hougne, P. Beyond-Diagonal Dynamic Metasurface Antenna. *IEEE Commun. Lett.* (2025).
71. del Hougne, P. A physics-compliant *diagonal* representation for wireless channels parametrized by *beyond-diagonal* reconfigurable intelligent surfaces. *IEEE Trans. Wirel. Commun.* **24**, 5871–5884 (2025).
72. Rahman, M. S. S., Yang, X., Li, J., Bai, B. & Ozcan, A. Universal linear intensity transformations using spatially incoherent diffractive processors. *Light Sci Appl* **12**, 195 (2023).
73. Li, H., Nerini, M., Shen, S. & Clerckx, B. A Tutorial on Beyond-Diagonal Reconfigurable Intelligent Surfaces: Modeling, Architectures, System Design and Optimization, and Applications. *IEEE Commun. Surv. Tutor.* **28**, 4086–4126 (2025).
74. Tapie, J., Nerini, M., Clerckx, B. & del Hougne, P. Beyond-Diagonal RIS Prototype and Performance Evaluation. *IEEE Wirel. Commun. Lett.* (2025).
75. Prod'homme, H. & del Hougne, P. Mutual Coupling in Dynamic Metasurface Antennas: Foe, but also Friend. *IEEE Wirel. Commun.* **32**, 30–36 (2025).
76. Prod'homme, H., Tapie, J., Le Magoarou, L. & del Hougne, P. Benefits of Mutual Coupling in Dynamic Metasurface Antennas. *IEEE Trans. Antennas Propag.* (2025).
77. Semmler, D., Nossek, J. A., Joham, M., Böck, B. & Utschick, W. Decoupling Networks and Super-Quadratic Gains for RIS Systems with Mutual Coupling. *IEEE Trans. Wirel. Commun.* (2025).
78. Nerini, M., Li, H. & Clerckx, B. Global Optimal Closed-Form Solutions for Intelligent Surfaces With Mutual Coupling: Is Mutual Coupling Detrimental or Beneficial? *IEEE Trans. Wirel. Commun.* (2025).
79. Zhang, L. *et al.* Space-time-coding digital metasurfaces. *Nat. Commun.* **9**, 4334 (2018).
80. Verde, F., Darsena, D. & Galdi, V. Rapidly Time-Varying Reconfigurable Intelligent Surfaces for Downlink Multiuser Transmissions. *IEEE Trans. Commun.* **72**, 3227–3243 (2024).
81. Chen, X. Q. *et al.* Integrated sensing and communication based on space-time-coding metasurfaces. *Nat. Commun.* **16**, 1836 (2025).
82. Wu, G.-B., Dai, J. Y., Cheng, Q., Cui, T. J. & Chan, C. H. Sideband-free space–time-coding metasurface antennas. *Nat. Electron.* **5**, 808–819 (2022).
83. Kuznetsov, A. D., Holopainen, J. & Viikari, V. Multifrequency system model for multiport time-modulated scatterers. *IEEE Trans. Antennas Propag.* (2025).
84. Mengu, D., Rivenson, Y. & Ozcan, A. Scale-, Shift-, and Rotation-Invariant Diffractive Optical Networks. *ACS Photonics* **8**, 324–334 (2021).

85. Mengu, D. *et al*. Misalignment resilient diffractive optical networks. *Nanophotonics* **9**, 4207–4219 (2020).
86. Shlezinger, N., Whang, J., Eldar, Y. C. & Dimakis, A. G. Model-Based Deep Learning. *Proc. IEEE* **111**, 465–499 (2023).
87. Tapie, J., Prod'homme, H., Imani, M. F. & del Hougne, P. Systematic Physics-Compliant Analysis of Over-the-Air Channel Equalization in RIS-Parametrized Wireless Networks-on-Chip. *IEEE J. Select. Areas Commun.* **42**, 2026–2038 (2024).
88. Zheng, P., Wang, R., Shamim, A. & Al-Naffouri, T. Y. Mutual Coupling in RIS-Aided Communication: Model Training and Experimental Validation. *IEEE Trans. Wireless Commun.* **23**, 17174–17188 (2024).
89. Sol, J., Prod'homme, H., Le Magoarou, L. & del Hougne, P. Experimentally realized physical-model-based frugal wave control in metasurface-programmable complex media. *Nat. Commun.* **15**, 2841 (2024).
90. del Hougne, P. Experimental Multiport-Network Parameter Estimation and Optimization for Multi-Bit RIS. *IEEE Wirel. Commun. Lett.* (2025).
91. Prod'homme, H. & del Hougne, P. Efficient Computation of Physics-Compliant Channel Realizations for (Rich-Scattering) RIS-Parametrized Radio Environments. *IEEE Commun. Lett.* **27**, 3375–3379 (2023).
92. Momeni, A. *et al*. Training of physical neural networks. *Nature* **645**, 53–61 (2025).
93. Li, Y., Chen, S., Gong, T. & Ozcan, A. Model-free optical processors using in situ reinforcement learning with proximal policy optimization. *Light Sci Appl* **15**, 32 (2026).
94. Skalli, A. *et al*. Model-free front-to-end training of a large high performance laser neural network. *arXiv.2503.16943* (2025).
95. Hughes, T. W., Minkov, M., Shi, Y. & Fan, S. Training of photonic neural networks through in situ backpropagation and gradient measurement. *Optica* **5**, 864 (2018).
96. Pai, S. *et al*. Experimentally realized in situ backpropagation for deep learning in photonic neural networks. *Science* **380**, 398–404 (2023).
97. Oguz, I. *et al*. Forward–forward training of an optical neural network. *Opt. Lett.* **48**, 5249 (2023).
98. Ma, Q. *et al*. Smart metasurface with self-adaptively reprogrammable functions. *Light Sci. Appl.* **8**, 98 (2019).
99. Hu, S. *et al*. Electromagnetic metamaterial agent. *Light Sci. Appl.* **14**, 12 (2025).
100. Miller, D. A. B. Self-configuring universal linear optical component [Invited]. *Photonics Res.* **1**, 1 (2013).
101. del Hougne, P., Fink, M. & Lerosey, G. Shaping Microwave Fields Using Nonlinear Unsolicited Feedback: Application to Enhance Energy Harvesting. *Phys. Rev. Appl.* **8**, 061001 (2017).
102. Tradonsky, C. *et al*. Rapid laser solver for the phase retrieval problem. *Sci. Adv.* **5**, eaax4530 (2019).

103. Ra'di, Y., Nefedkin, N., Popovski, P. & Alù, A. Nonlinear, Active, and Time-Varying Metasurfaces for Wireless Communications: A perspective and opportunities. *IEEE Antennas Propag. Mag.* **66**, 52–62 (2024).
104. Leshno, M., Lin, V. Ya., Pinkus, A. & Schocken, S. Multilayer feedforward networks with a nonpolynomial activation function can approximate any function. *Neural Netw.* **6**, 861–867 (1993).
105. Ning, Y. M. *et al*. Multilayer nonlinear diffraction neural networks with programmable and fast ReLU activation function. *Nat Commun* **16**, 10332 (2025).
106. Brooker, G. & Gomez, J. Lev Termen's Great Seal bug analyzed. *IEEE Aerosp. Electron. Syst. Mag.* **28**, 4–11 (2013).
107. Li, Y., Li, J. & Ozcan, A. Nonlinear encoding in diffractive information processing using linear optical materials. *Light Sci. Appl.* **13**, 173 (2024).
108. Nerini, M. & Clerckx, B. Analog Computing for Signal Processing and Communications – Part I: Computing With Microwave Networks. *IEEE Trans. Signal Process.* **73**, 5183–5197 (2025).
109. Laporte, F., Katumba, A., Dambre, J. & Bienstman, P. Numerical demonstration of neuromorphic computing with photonic crystal cavities. *Opt. Express* **26**, 7955 (2018).
110. Tymchenko, M., Sounas, D., Nagulu, A., Krishnaswamy, H. & Alù, A. Quasielectrostatic Wave Propagation Beyond the Delay-Bandwidth Limit in Switched Networks. *Phys. Rev. X* **9**, 031015 (2019).
111. Liaskos, C., Katsalis, K., Triay, J. & Schmid, S. Resource Management for Programmable Metasurfaces: Concept, Prospects and Challenges. *IEEE Commun. Mag.* **61**, 208–214 (2023).
112. Ma, R., Qiu, L. & Hu, W. SurfOS: Towards an Operating System for Programmable Radio Environments. *Proc. ACM HOTNETS* 132–141 (2024).

Acknowledgements

P.d.H. acknowledges support from the Nokia Foundation (20260028) and the French National Agency for Research (ANR-22-PEFT-0005, ANR-22-CE93-0010).

T.J.C. acknowledges support from the National Natural Science Foundation of China (62288101).

A.O. acknowledges support from the U.S. Department of Energy (DOE), Office of Basic Energy Sciences, Division of Materials Sciences and Engineering (DE-SC0023088).